International Journal of Environmental Sciences
ISSN: 2229-7359
Vol. 11 No. 23s, 2025
https://www.theaspd.com/ijes.php

Numerical Investigation Of A Refrigerant Ejector: Effect Of Ejector Geometry

L.S. Aurangabadkar[1], S. Chaudhary[2]
[1]Institute of Engineering and Technology, Devi Ahilya Vishwavidyalaya, lokeshsaurangabadkar@gmail.com
[2]Khandwa Road Indore-452017 (M.P.), India, schaudhary@ietdavv.edu.in

Abstract– *Ejectors have gained extensive utilization in refrigeration and air-conditioning systems recently, due to their simple design, minimal maintenance, and diminished expansion losses. The ejector performance is markedly sensitive to geometric configurations and refrigerant characteristics. The current study presents a numerical investigation into the performance of a two-phase ejector by varying the geometrical parameters. Computational Fluid Dynamics (CFD) analysis was carried out to examine the flow dynamics within the ejector and its performance under a predetermined set of operational conditions. Parametric values from previously published scholarly works were employed and modified in the present investigation with the objective of enhancing the overall ejector performance. The primary nozzle convergence and divergence angles, as well as the secondary nozzle convergence and divergence angles, were altered, and their impact on flow and overall efficiency was evaluated. This numerical inquiry furnishes significant insights for ejector design and its performance. The findings will further augment the advancement of more sustainable and energy-efficient refrigeration systems.*

Keywords: *Ejector, Refrigeration System, Computational Fluid Dynamics.*

INTRODUCTION

Ejectors are among the simplest fluid devices since they operate without moving parts, seals, or lubricants. This inherent simplicity makes them highly reliable, with low initial and maintenance costs, which explains their extensive use in chemical and energy-related processes.

Huang et al. [1] developed a one-dimensional model to predict ejector performance under critical operating conditions, assuming constant-pressure mixing. Their study, which involved testing eleven ejectors with R141b, demonstrated that the inclusion of empirical coefficients significantly improved prediction accuracy, with results closely aligning with experimental data. They concluded that the 1-D framework provides a practical and reliable method for evaluating ejector behavior.

Building on this, Scott et al. [2] applied Computational Fluid Dynamics (CFD) with real-gas properties to investigate supersonic ejectors. Their simulations, validated using experimental results with R141b and R245fa, showed an error margin of less than 11%. The study highlighted the influence of geometric parameters such as nozzle exit position, mixing length, and evaporator inlet diameter on performance, identifying conditions that optimize ejector efficiency. These findings reinforced CFD as a robust tool for ejector design and optimization.

Similarly, Besagni et al. [3] conducted a comprehensive validation of CFD models for single-phase supersonic ejectors across different working fluids, geometries, and operating conditions. Their work emphasized best practices for numerical modeling, including grid resolution, aspect ratio, near-wall treatment, and mesh refinement. Interestingly, they found minimal differences between two- and three-dimensional models, with pressure-based solvers offering faster convergence. Among turbulence models, the k–ω SST approach was shown to provide the best accuracy, establishing a reliable reference for future CFD studies on ejectors.

D. hu et al. [4] proposed a central annular slit ejector structure as a promising alternative to conventional designs. the high-pressure fluid is discharged through an annular nozzle, entraining low-pressure fluid simultaneously from both the inner and outer sides of the jet. Detailed CFD simulations coupled with entropy generation analysis demonstrated that the annular design not only lowers entropy generation across

different operating conditions but also promotes more uniform velocity distributions and shortens the mixing section length.

Beyond geometry modifications, multi-stage and hybrid modeling approaches have also been explored. Suvarnakuta et al. [5] investigated a two-stage ejector (TSE) with an annular secondary inlet using CFD. Their optimized design achieved up to a 77.2% increase in entrainment ratio compared with single-stage ejectors, although at the cost of a slight reduction in critical back pressure. These findings point to the potential of multi-stage arrangements for improving refrigeration efficiency, though experimental confirmation is still needed. Marum et al. [6] combined a quasi-one-dimensional model with CFD for water ejectors, enabling friction losses and efficiency characteristics to be derived directly from simulations and then validated experimentally. Their work also compared turbulence models, concluding that the k–ω SST closure delivered the most reliable predictions. Importantly, they observed that efficiency estimation is strongly influenced by boundary-layer resolution at high entrainment ratios and by velocity profile accuracy at low entrainment ratios.

Bumrungthaichaichan et al. [7] provided further insights by comparing ejectors designed under constant rate of momentum change (CRMC) and constant pressure mixing (CPM) assumptions using CFD with the SST k–ω turbulence model. Their results, which matched well with experimental data, showed that CRMC ejectors generally achieved higher entrainment ratios but lower critical condenser pressures compared with CPM ejectors. Notably, when the primary expansion coefficient exceeded unity, CRMC ejectors reached efficiency improvements of up to 32.4%, outperforming CPM counterparts under those conditions.

A. Rumane et al. [8] conducted a comprehensive CFD investigation of ejector systems, offering detailed insights into flow behavior and performance prediction. Extending this line of research, Hadi et al. [9] analyzed ejectors operating with different refrigerants, including pentane, propane, butane, iso-butane, R1234ze, and R1234yf. Their work highlighted key internal flow features such as shockwave formation, boundary-layer separation, and vortex dynamics, which play a critical role in determining ejector efficiency. Similarly, Mohamed et al. [10] employed the NIST real gas model to simulate ejector performance and concluded that smaller area ratios favor higher compression ratios, underscoring the strong influence of geometric parameters on system performance.

Beyond refrigeration, ejector technology has also been applied in combustion systems. Tong et al. [11] designed an industrial burner incorporating multiple ejectors to reduce nitrogen oxide emissions. Using CFD coupled with orthogonal analysis, they optimized premixing behavior and tested cylindrical and rectangular flue configurations. Among the designs, the R2 and C1 burners achieved the best temperature uniformity, with the optimized R2 model delivering excellent premixing and combustion characteristics while satisfying industrial denitration requirements.

From a refrigerant perspective, R1234yf (2,3,3,3-tetrafluoropropene) has gained prominence as a fourth-generation, low-global-warming-potential (GWP) alternative to traditional refrigerants. Its thermophysical properties make it particularly suitable for ejector-based cooling systems, where compression is achieved using low-grade thermal energy rather than electricity. This positions R1234yf as a promising working fluid for sustainable and environmentally friendly refrigeration applications.

K. Abbady et. al [12], has focused on variable-geometry ejectors to overcome the limitations of fixed designs under fluctuating operating conditions. Using R1234yf as the working fluid, a CFD model was developed to evaluate a Variable Geometry Ejector (VGE) equipped with a movable spindle and adjustable nozzle exit position. Results showed that when the primary temperature was below the optimal threshold, the best performance was achieved with the nozzle exit at 0 mm, whereas higher or optimal primary temperatures benefited from a negative nozzle exit position, improving entrainment ratio and raising critical temperatures by up to 11.8%. While ejectors without a spindle achieved higher entrainment ratios, their stable operating range was narrower. Incorporating a spindle at 0 mm notably increased the critical temperature by 25.8%. A Design of Experiment (DOE) analysis identified the most influential operating and geometric parameters, and an artificial neural network successfully predicted entrainment ratios with high accuracy (R^2 = 99.81%).

Yu et al. [13] introduced a gas-dynamic design method for R1234yf ejectors, focusing on optimizing the area ratio (AR) and nozzle exit position (NXP) using control variable algorithms. Their simulations revealed that the entrainment ratio initially increases and then decreases with rising AR and NXP. While AR was found to strongly influence shockwave position within the mixing chamber, NXP directly governed the expansion of the motive fluid, making both parameters critical for enhancing ejector performance.

Suresh et al. [14] numerically evaluated five low-GWP alternatives to R134a across a range of ARs and NXPs. Among them, R1234yf and R1243zf consistently delivered the highest entrainment ratios, with larger ARs further boosting performance. Similarly, Sharma and Sachdeva [15] carried out a one-dimensional ejector analysis using R1234yf and R1234ze, reporting COP improvements of 40.98% and 6.63%, respectively, when the generator superheat increased from 2 °C to 6 °C. These findings highlight the combined importance of refrigerant selection and geometric design parameters in improving ejector efficiency.

In another development, Liu et al. [16] proposed an ejector-expansion refrigeration cycle (EERC) incorporating two evaporating temperatures to recover partial expansion work. Using refrigerant mixtures of R1234yf, R1234ze, and R152a, the EERC achieved 17.1% higher COP and 16.4% higher exergy efficiency compared with conventional bi-evaporator systems, while total exergy losses were reduced by 26.1%. This demonstrated the potential of optimized cycle configurations in enhancing both energy and exergy performance.

Several other studies [17–19] have likewise emphasized the promise of R1234yf as an environmentally friendly alternative to high-GWP refrigerants such as R134a, reinforcing its suitability for future ejector-based refrigeration applications.

EJECTOR REFRIGERATION SYSTEM

The system investigated in this study was originally proposed by D. Scott (2008), as shown in Fig. 1(a). In an ejector refrigeration cycle, the motive fluid is heated at constant pressure in the generator (7–0) and expanded through the primary nozzle, inducing suction in the suction chamber. The secondary fluid from the evaporator (point 6) is entrained and mixed with the primary flow in the ejector. The mixed stream then expands to an intermediate pressure and enters the condenser (point 3), where it condenses and exits as liquid (point 5). The condensate is split into two streams: one directed back to the generator (5–7), and the other expanded through a valve (5–6) before re-entering the evaporator (point 6), completing the cycle.

Ejectors are typically classified by nozzle exit location [1]. In constant-area mixing ejectors, the nozzle exit lies within the constant-area section, and mixing occurs entirely in this region. In constant-pressure mixing ejectors, the nozzle exit is located in the suction chamber, where the streams mix under uniform pressure. The latter design generally exhibits superior performance and is more commonly adopted.

This work investigates a constant-pressure ejector but proposes a modified configuration in which mixing extends into the constant-area section. The constant-pressure mixing theory, widely applied in ejector modeling [1,4,5], assumes equal exit pressures for the primary and secondary streams, with mixing occurring at constant pressure up to the entrance of the constant-area section.

In practice, ejector operation is governed by two distinct choking phenomena [6,7]:

- Primary flow choking, which occurs within the converging–diverging nozzle; and
- Secondary flow choking, which arises as the entrained stream accelerates from near-stagnation at the suction port to supersonic velocities in the constant-area section.

Fig. 2 illustrates the variation of the entrainment ratio with discharge (back) pressure P_c at fixed suction pressure P_e and primary flow pressure P_g. Based on P_c, ejector performance can be divided into three operating regimes:

- Critical mode (double-choking, $P_c \leq P_{c*}$): Both primary and secondary flows are choked, and the entrainment ratio remains constant at its maximum value.
- Subcritical mode (single-choking, $P_{c*} < P_c \leq P_{co}$): Only the primary flow is choked, and the entrainment ratio decreases with increasing P_c.

- Malfunction mode (backflow, $P_c > P_{co}$): Neither stream is choked, and reverse flow occurs in the secondary passage, causing the entrainment ratio to drop to zero.

For efficient operation, ejectors are preferably designed to operate in the critical mode, where both flows are choked and the maximum entrainment ratio is sustained.

The present study develops a performance model specifically for critical-mode operation, with constant-pressure mixing assumed within the constant-area section and secondary flow choking explicitly considered. Refrigerant R1234yf is adopted as the working fluid under a defined set of operating conditions. To address the limited understanding of how nozzle geometries influence ejector behaviour, this work investigates the effect of varying the convergence and divergence angles of both the primary and secondary nozzles. The findings aim to provide new insights into the geometric optimization of ejectors for enhanced performance.

EJECTOR PERFORMANCE ANALYSIS

Governing Equations and Thermodynamics

The ejector expansion system consists of two thermodynamic cycles, one being the power cycle (7-0-1-3-5-7) and other the refrigeration cycle (6-4-1-3-5-6). The working fluid is same in both the cycles. Fig. 1(b).

Considering all the processes to be reversible and adiabatic the thermodynamic analysis is carried out.

Heat added to working fluid in the generator (Q_g)

$$Q_g = m_1.(h_0 - h_7) \quad (1)$$

The refrigeration capacity (Q_e)

$$Q_e = m_2.(h_4 - h_6) \quad (2)$$

The Pump work (W_p)

$$W_p = m_1.(h_7 - h_5) \quad (3)$$

The total coefficient of performance

$$COP = \frac{\mathrm{Qe}}{(\mathrm{Qg} + \mathrm{Wp})} \quad (4)$$

The energy equation for ejector control volume

$$m_1.h_0 + m_2.h_4 = (m_1 + m_2).h_3 \quad (5)$$

The entrainment ratio is defined as mass flow rate of secondary flow m_2 to the mass flow rate of primary fluid flow m_1.

$$\omega = \frac{m_2}{m_1} \quad (6)$$

The coefficient of performance in terms of entrainment ratio is given by

$$COP = \frac{\omega\,(h_4 - h_6)}{(h_0 - h_5)}$$

Assuming throttling process to be isenthalpic hence $h_5 = h_6$

$$COP = \frac{\omega\,(h_4 - h_5)}{(h_0 - h_5)} \quad (7)$$

Since these enthalpies are function of evaporator, generator and condenser temperature. The COP can be calculated by equation (7).

COMPUTATIONAL METHODOLOGY

Computational Fluid Dynamics (CFD) has become a widely adopted tool for the design and analysis of fluid dynamic systems. In the present study, the ejector geometry proposed by Huang et al. [1] is employed as the baseline design. The key geometric specifications are summarized in Table 1 , while the schematic of the ejector is shown in Fig. 2.

The simulations are carried out using ANSYS 16.2, where the ejector geometry is modeled and meshed, and ANSYS Fluent is employed as the CFD solver. An axisymmetric model is adopted to reduce computational effort while preserving flow characteristics. The working fluid selected for this study is R1234yf, modeled as an ideal gas during the simulations.

The boundary conditions, solution setup, and other solver specifications are outlined in Table 2.

MATHEMATICAL MODEL

In ejector performance analysis, the flow field is governed by the fundamental conservation laws of mass, momentum, and energy. Since the working fluid within the ejector frequently accelerates to supersonic velocities, the compressible, axisymmetric Navier–Stokes equations are employed to model the variable-pressure flow behavior.

In this study, the governing equations are solved using a pressure-based implicit solver. Although density-based solvers are often applied for high-speed compressible flows, the pressure-based formulation is more suitable for ejector applications, as it effectively handles combined subsonic–supersonic regions and strong pressure gradients while maintaining numerical stability. This approach has been widely validated in ejector flow simulations and ensures reliable convergence under the present operating conditions.The mathematical formulation of these equations is presented as follows:

Continuity Equation

$$\frac{\partial \rho}{\partial t} + \nabla . (\rho v) = 0 \quad (8)$$

Momentum Conservation Equation

$$\frac{\partial (\rho v)}{\partial t} + \nabla \cdot (\rho v . v) = -\nabla p + \nabla \cdot \tau + \rho g \quad (9)$$

Energy Equation

$$\frac{\partial (\rho E)}{\partial t} + \nabla \cdot \left(v (\rho E + p) \right) = \nabla \cdot \left(k_{eff} \nabla T - \sum h_j . J_j + (\tau \cdot v) \right) + Sh \quad (10)$$

where

- v = velocity vector
- p = static pressure
- τ = viscous stress tensor
- g = gravitational acceleration vector
- E = total energy per unit mass
- k_{eff} = effective thermal conductivity
- J_j = diffusive flux of species j
- S_h = volumetric heat source

In pressure-based implicit solver, these equations are discretized using a coupled or segregated approach.
For constant-pressure or low-Mach number flows, density is typically obtained from an equation of state or assumed constant, with pressure primarily enforcing continuity rather than driving compressibility effects. In compressible ejector flows, however, the same formulation is applied with density variations computed from pressure and temperature through the ideal gas law (or an appropriate equation of state).
Turbulence effects play a crucial role in ejector performance, particularly in predicting jet mixing and shock–shear interactions. In this study, turbulence is modelled using the standard k–ε model developed by Launder and Spalding, which solves transport equations for turbulent kinetic energy k and its dissipation rate ε. This model offers a good compromise between computational efficiency and accuracy, making it suitable for capturing the supersonic mixing regions characteristic of ejector flows. The transport equations can be expressed as:

$$\frac{\partial (\rho k)}{\partial t} + \frac{\partial (\rho k u_j)}{\partial x_j} = \frac{\partial \left[\left(\mu + \frac{\mu_t}{\sigma_k}\right).\frac{\partial_k}{\partial x_j}\right]}{\partial x_j} + G_k - \rho.\varepsilon \quad (11)$$

$$\frac{\partial (\rho \varepsilon)}{\partial t} + \frac{\partial (\rho \varepsilon u_j)}{\partial x_j} = = \frac{\partial \left[\left(\mu + \frac{\mu_t}{\sigma_\varepsilon}\right).\frac{\partial \varepsilon}{\partial x_j}\right]}{\partial x_j} + C_{1_\varepsilon}.\frac{\varepsilon}{k}.G_k - C_{2_\varepsilon}.\rho\,\varepsilon^2/k \quad (12)$$

Where:

- ρ = fluid density
- u_j = mean velocity in the j - direction
- μ = molecular viscosity
- μ_t = turbulent viscosity
- G_k = production of turbulent kinetic energy due to mean velocity gradients
- Model constants (standard values): [5]

C_μ = 0.09, $C_{1\varepsilon}$ = 1.44, $C_{2\varepsilon}$ = 1.92, σ_k = 1.0, σ_ε = 1.3

METHODOLOGY

Geometry and Meshing

An axisymmetric ejector geometry, comprising the primary nozzle, constant-area mixing section, and diffuser, was developed in ANSYS 16.2 Design Modeler based on the reference design. The computational domain was discretized with a structured mesh to ensure accuracy while maintaining computational efficiency (mesh details shown in Fig. 3). A grid-independence test was conducted by comparing entrainment ratios across progressively refined meshes. The mesh density was finalized when further refinement produced less than 1% variation in performance parameters.

Boundary Conditions

The primary and secondary inlet pressures and temperatures were prescribed according to the design operating conditions, while the outlet was fixed at the condenser pressure. All boundary conditions are summarized in Table 3.

Numerical Setup

The compressible, axisymmetric Navier–Stokes equations were solved in ANSYS Fluent using the finite volume method with a pressure-based implicit solver. Turbulence was modeled using the standard k–ε model, which provides a good compromise between computational cost and predictive accuracy in supersonic ejector flows. Mass, momentum, and energy conservation equations were applied, and convergence was ensured through residual reduction below 10^{-5} and global mass balance checks.

Validation

The numerical model was validated by comparing simulation results with the experimental data reported by Huang et al. [1]. The predicted entrainment ratios and pressure distributions showed good agreement with published results, confirming the reliability of the adopted computational approach.

Performance Evaluation

- Simulations were carried out using R1234yf as the working fluid, modelled as an ideal gas. Flow characteristics were analysed through contour plots of pressure, velocity, Mach number, density, and temperature. Ejector performance was assessed by evaluating the entrainment ratio and coefficient of performance (COP) under different geometric configurations.
- Optimization of Primary Nozzle Convergence Angle

The refrigerant system was simulated with varying Primary Nozzle Convergence Angle. COP was evaluated for each case, and the optimal angle was identified.

- Optimization of Primary Nozzle Divergence Angle

The refrigerant system was simulated with varying Primary Nozzle Divergence Angle. COP was evaluated for each case, and the optimal angle was identified.

- Optimization of Secondary Nozzle Convergence Angle

The refrigerant system was simulated with varying Secondary Nozzle Convergence Angle. COP was evaluated for each case, and the optimal angle was identified.

- Optimization of Secondary Nozzle Divergence Angle

The refrigerant system was simulated with varying Secondary Nozzle Divergence Angle. COP was evaluated for each case, and the optimal angle was identified.

RESULTS AND DISCUSSION

PART - 1 Primary Nozzle Convergence Angle Variation

The effect of varying the primary nozzle convergence angle on ejector performance is analysed in terms of entrainment ratio and coefficient of performance (COP). The results are summarized in Table 4 and represented graphically in plot 4.

It is evident that both entrainment ratio and COP are sensitive to changes in convergence angle. At smaller angles (14.72°–15.72°), the entrainment ratio gradually decreases from 0.792 to 0.774, accompanied by a corresponding drop in COP from 0.734 to 0.721. This trend can be attributed to reduced mixing effectiveness between the motive and suction flows at lower nozzle expansion, which limits the entrainment capacity.

Interestingly, at a convergence angle of 16.22°, a clear performance enhancement was observed, where the entrainment ratio reached its maximum value of 0.839, with COP also peaking at 0.738. This suggests that the nozzle angle at this condition provides an optimum balance between jet expansion and mixing, minimizing flow separation and shock-induced losses within the ejector.

Beyond this point, further increases in convergence angle (16.72°–17.72°) led to a sharp decline in both entrainment ratio and COP. For instance, at 17.72°, the entrainment ratio dropped to 0.748 and COP

reduced to 0.691, indicating that excessive convergence hinders flow entrainment due to increased flow resistance and unfavourable shock structures in the mixing chamber.
Overall, the results highlight that an optimum convergence angle exists around 16.22°, where both entrainment ratio and COP are maximized. This emphasizes the strong dependence of ejector performance on nozzle geometry and confirms the importance of careful optimization to achieve energy-efficient operation.

PART - 2 Primary Nozzle Divergence Angle Variation

The influence of primary nozzle divergence angle on ejector performance is investigated, with the corresponding entrainment ratio and COP values summarized in Table 5 and represented graphically in plot 5.
The results indicate a strong dependence of system performance on nozzle divergence angle. At small divergence angles, both entrainment ratio and COP exhibited favourable values. Specifically, at 2°, the entrainment ratio reached a peak of 1.134, with COP attaining a maximum of 1.090, representing the optimal performance condition among the tested cases. This improvement can be attributed to enhanced expansion and mixing of the motive jet at moderate divergence, which promotes effective entrainment of the secondary flow.
As the divergence angle increased beyond 2°, a noticeable decline in performance was observed. At 2.5°, both entrainment ratio and COP decreased slightly (0.997 and 1.020, respectively), and further reductions were recorded at 3° (0.839 and 0.788). This downward trend suggests that excessive divergence weakens jet momentum and induces flow instabilities such as shock formation and boundary layer separation, thereby reducing entrainment capability.
A dramatic drop in performance occurred at divergence angles above 3.5°. At 3.5°, the entrainment ratio fell sharply to 0.270 and COP to 0.280, indicating significant flow breakdown. For even higher divergence angles (4°–4.5°), the entrainment ratio and COP values turned negative, highlighting unstable operation and reverse flow phenomena within the ejector. Such results confirm that the nozzle diverging section becomes highly unfavourable at large angles due to severe separation and energy losses.
Overall, the analysis demonstrates that an optimum divergence angle exists around 2°, where the ejector achieves maximum entrainment ratio and COP. Both smaller and larger angles deviate from this optimum, either due to insufficient expansion or excessive divergence leading to instability. This finding reinforces the critical role of nozzle divergence angle in ejector design and highlights the necessity of precise geometric optimization to ensure stable and efficient operation.

PART - 3 Secondary Nozzle Convergence Angle Variation

The variation of secondary nozzle convergence angle and its influence on ejector performance were analyzed, with the corresponding entrainment ratio and COP values provided in Table 6 and plot 6.
At lower convergence angles (11°–13°), both entrainment ratio and COP showed relatively modest values, gradually decreasing with increasing angle. For instance, at 11°, the entrainment ratio was 0.770 with a COP of 0.719, whereas at 13°, these values reduced slightly to 0.752 and 0.702, respectively. This indicates that at smaller convergence angles, the nozzle expansion is insufficient to promote effective mixing, thereby limiting entrainment.
A significant improvement was observed at a convergence angle of 14°, where both performance parameters reached their maximum values. The entrainment ratio increased to 0.839, and COP peaked at 0.788, suggesting that this angle provides the optimum balance between flow acceleration and mixing efficiency in the ejector. The results imply that at this geometry, flow separation is minimized, and favorable shock structures are formed, leading to enhanced entrainment and system efficiency.
Beyond the optimum point, further increases in the secondary convergence angle led to a decline in performance. At 15° and 16°, entrainment ratio and COP values reduced to 0.836/0.776 and 0.804/0.736, respectively, though performance remained higher than at the lowest tested angles. At 17°, however, a sharp

reduction in COP was noted (0.626), despite an entrainment ratio of 0.785, indicating unstable operation and higher irreversibility's at larger nozzle angles.
Overall, the analysis confirms that ejector performance is highly sensitive to secondary nozzle convergence angle, with an optimum around 14°, where entrainment ratio and COP are maximized. Angles smaller or larger than this optimum result in reduced efficiency due to either insufficient jet expansion or excessive divergence-induced losses.

PART - 4 Secondary Nozzle Divergence Angle Variation

The impact of secondary nozzle divergence angle on ejector performance was evaluated in terms of entrainment ratio and COP (Table 7) and plot 7.
At lower divergence angles (2°–3°), both entrainment ratio and COP exhibited a steady upward trend. Specifically, the entrainment ratio increased from 0.747 at 2° to 0.823 at 3°, while the COP rose from 0.701 to 0.773. This improvement suggests that moderate divergence promotes smoother jet expansion and enhances mixing efficiency within the ejector.
Further enhancement was observed at 3.5°–4.5°, where performance reached near-optimal levels. At 4°, the entrainment ratio peaked at 0.844 with a corresponding COP of 0.792, and a similar value was recorded at 4.5°. This indicates that the ejector operates most efficiently within this range, as the divergent section effectively guides the flow while avoiding major separation losses.
However, when the divergence angle was increased further to 5°, a dramatic deterioration in performance was observed. The entrainment ratio dropped sharply to 0.415, and COP fell drastically to 0.239. This sharp decline can be attributed to excessive divergence, which leads to severe flow separation, vortex formation, and shock-induced irreversibilities, thereby undermining entrainment capacity and refrigeration efficiency.
In summary, the results clearly indicate that the optimum secondary nozzle divergence angle lies between 3.5° and 4.5°, where both entrainment ratio and COP are maximized. Angles below this range result in incomplete jet expansion and weaker mixing, whereas larger divergence angles lead to flow instability and significant performance degradation.

CONCLUSION AND FUTURE SCOPE

The present work highlights the computational fluid dynamic analysis of an ejector. Under a specified set of operating conditions. ejector was tested with refrigerant R1234yf.
To find the effects of geometric parameters on ejector performance seven different Primary nozzle convergence angle values were identified. COP was calculated and the convergence angle value with highest values of COP is obtained. Same process is repeated for seven different Primary Nozzle divergence angles, Secondary Nozzle Convergence and divergence angles and optimum values of these geometric parameters has been obtained.
The present study can be extended further by variation in meshing methods, using different turbulence models, varying the operating conditions and changing geometric parameters like mixing section length, diameter and nozzle exit position etc.

CONFLICT OF INTEREST

The authors declare that they have no conflicts of interest.

REFERENCES

[1] B.J. Huang, J.M. Chang, C.P. Wang, V.A. Petrenko. "A 1-D analysis of ejector performance," International Journal of Refrigeration 22 (1999) 354 - 364. https://doi.org/10.1016/S0140-7007(99)00004-3.
[2] D. Scott, Z. Aidoun, O. Bellache, M. Ouzzane. "CFD Simulations of a Supersonic Ejector for Use in Refrigeration Applications." International Refrigeration and Air Conditioning Conference, Purdue university, July 14-17, 2008. https://docs.lib.purdue.edu/cgi/viewcontent.cgi?article=1926&context=iracc.

[3] G. Besagni, N. Cristiani, L. Croci, G. Raymond Guédon, F. Inzoli. "Computational fluid-dynamics modelling of supersonic ejectors: screening of modelling approaches, comprehensive validation and assessment of ejector component efficiencies." Applied Thermal Engineering, Volume **186**, 5 March 2021, 116431. https://doi.org/10.1016/j.applthermaleng.2020.116431
[4] D. Hu, G. Chen, Y. Zhao, D. Jiang. "A novel central annular slit ejector: Flow characteristics analysis and experimental performance investigation." International Journal of Heat and Mass Transfer, Volume **254,** 2026, 127636. https://doi.org/10.1016/j.ijheatmasstransfer.2025.127636.
[5] N. Suvarnakuta, K. Pianthong, T. Sriveerakul, W. Seehanam, "Performance analysis of a two-stage ejector in an ejector refrigeration system using computational fluid dynamics." Engineering Applications of Computational Fluid Mechanics, Volume **14**, 2020, 669-682. https://doi.org/10.1080/19942060.2020.1756913.
[6] V. Marum, L. Reis, F. Maffei, S. Ranjbarzadeh, I. Korkischko, R. Gioria, J. Meneghini. "Performance analysis of a water ejector using Computational Fluid Dynamics (CFD) simulations and mathematical modeling." Energy, Volume **220**, 1 April 2021, 119779. https://doi.org/10.1016/j.energy.2021.119779.
[7] E. Bumrungthaichaichan, N. Ruangtrakoon, T. Thongtip. "Performance investigation for CRMC and CPM ejectors applied in refrigeration under equivalent ejector geometry by CFD simulation." Energy Reports, Volume **8**, November 2022, Pages 12598-12617. https://doi.org/10.1016/j.egyr.2022.09.042.
[8] A. Rumane, S. Mondkar (2023). Performance Optimization of Steam Ejector Using CFD Analysis. In: Vasudevan, H., Kottur, V.K.N., Raina, A.A. (eds) Proceedings of International Conference on Intelligent Manufacturing and Automation. Lecture Notes in Mechanical Engineering. Springer, Singapore. Performance Optimization of Steam Ejector ++++Using CFD Analysis | SpringerLink.
[9] M. Hadi, A. Arshad, N. Basha Shaik, W. Benjapolakul, Q. Fatima Gillani. "Optimization Of Hydrocarbon Ejector Using Computational Fluid Dynamics." Regular Issue / Environment, Energy and Natural Resources, Vol. **26** No. 5 (2022). DOI:10.4186/ej.2022.26.5.1.
[10] S. Mohamed, Y. Shatilla, T. Zhang. "CFD-based design and simulation of hydrocarbon ejector for cooling." Energy, Volume **167**, 15 January 2019, Pages 346-358. https://doi.org/10.1016/j.energy.2018.10.057.
[11] C. Tong, Z. Chen, X. Chen, Q. Xie. "Research and Development of an Industrial Denitration-Used Burner with Multiple Ejectors via Computational Fluid Dynamics Analysis." Mathematics 2023, *11*(16), 3476. https://doi.org/10.3390/math11163476.
[12] K. Abbady, N. Al-Mutawa, A. Almutairi . "The performance analysis of a variable geometry ejector utilizing CFD and artificial neural network." Energy Conversion and Management, Volume **291**, September 2023, 117318. https://doi.org/10.1+++++016/j.enconman.2023.117318.
[13] M. Yu, C. Wang, L. Wang, H. Zhao. "Optimization Design and Performance Evaluation of R1234yf Ejectors for Ejector-Based Refrigeration Systems." *Entropy* 2022, *24*(11), 1632. https://doi.org/10.3390/e24111632.
[14] R.Suresh, R.Prakash, V.Praveen, S.Datta. "Numerically Optimized Ejector Geometry for Ejector Refrigeration Systems With Low-Global Warming Potential Working Fluids." ASME Journal of Energy Resources Technology, Volume **146**, October 2024, 101702. https://doi.org/10.1115/1.4065729.
[15] B. Sharma and G. Sachdeva. "Performance and Dimensions Determination of an Ejector Utilized in Ejector Cooling Cycle with Eco-Friendly Working Fluids." EVERGREEN Joint Journal of Novel Carbon Resource Sciences & Green Asia Strategy, Vol. **10**, Issue 03, pp1460-1478, September 2023. https://doi.org/10.5109/7151695.
[16] N. Khaldi, S. Sdiri, M. Lazaar. "Thermodynamic analysis and optimization of an ejector refrigeration system for sustainable cooling applications." International Journal of Refrigeration, 2025, **174,** 372-387. https://doi.org/10.1016/j.ijrefrig.2025.03.004.
[17] A. Elbarghthi, M. Hdaib, V. rák. "ANovelGenerator Design Utilised for Conventional Ejector Refrigeration Systems." Energies 2021, **14**, 7705. https://doi.org/10.3390/en14227705.
[18] B. Zohbia, N. Bukharinb, H. Assoumc, K. Meraima, A. Sakouta, M. Hassand, "Investigation of the effects of the jet nozzle geometry and location on the performance of supersonic fluid ejectors." Energy Reports, Volume **8**, Supplement 3, June 2022, Pages 228-233. https://doi.org/10.1016/j.egyr.2022.01.029.
[19] Q. Liu, Zengshi Xu, A. Wang, Z. Ping, L. Wang. "Weight analysis on geometric parameters of ejector under high back pressure condition of SOFC recirculation system." International Journal of Hydrogen Energy, Volume **47**, Issue 63, 26 July 2022, Pages 27150-27165. https://doi.org/10.1016/j.ijhydene.2022.06.069.

TABLES

Ejector Part Name	Notation	Length in mm
Primary Nozzle Assembly Length	H1	40
Primary Nozzle Convergence Length	H8	18.32
Primary Nozzle Divergence Length	H9	18.32
Primary Nozzle Inlet diameter	V10	6.65
Secondary Nozzle Convergence Length	H2	32.24
Secondary Nozzle Mixing Section Length	H3	35.6
Secondary Nozzle Divergence Length	H4	56.94
Ejector exit diameter	V7	7.04

Table 1

S.No.	Boundary Condition	Value
1	Generator Pressure	400600 Pa
2	Evaporator Pressure	39990 Pa
3	Condenser Pressure	60000 Pa
4	Primary Nozzle Inlet Temperature	351 K
5	Secondary Nozzle Inlet Temperature	281 K
6	Ejector Exit Temperature	294 K
7	Entrainment Ratio	0.415216

Table 3

S.No.	Numerical Model Criteria	Selected Criteria
1	Domain	Axisymmetric
2	Boundary Conditions at Inlet	Pressure Based
3	Boundary Conditions at Outlet	Pressure Based
4	Meshing Information	Structured Quadrilateral Elements with 10396 Nodes and 9960 Elements.
5	Solver Type	Simple-implicit
6	Turbulence Model	Std. K-Epsilon
7	Wall Treatment Method	Std. Wall Function

Table 2

S.No.	Primary Nozzle Convergence Angle (degree)	Entrainment Ratio	COP
1	14.72	0.792462	0.73438
2	15.22	0.790777	0.730266
3	15.72	0.773507	0.721321
4	16.22	0.839187	0.738292
5	16.72	0.743367	0.693304
6	17.22	0.741826	0.691260
7	17.72	0.747689	0.690569

Table 4

S.No.	Primary Nozzle Divergence Angle (degree)	Entrainment Ratio	COP
1	1.5	0.861536	0.653215
2	2	1.13444	1.09034
3	2.5	0.997414	1.01992
4	3	0.839187	0.787737
5	3.5	0.270398	0.279823
6	4	-0.829216	-0.945987
7	4.5	-0.64276	-0.755648

Table 5

S.No.	Secondary Nozzle Convergence Angle (degree)	Entrainment Ratio	COP
1	11	0.769825	0.719099
2	12	0.75986	0.709549
3	13	0.751782	0.701887
4	14	0.839187	0.788464
5	15	0.835856	0.77595
6	16	0.804041	0.735919
7	17	0.784893	0.625581

Table 6

S.No.	Secondary Nozzle Divergence Angle (degree)	Entrainment Ratio	COP
1	2	0.747126	0.70132
2	2.5	0.795226	0.746471
3	3	0.823248	0.772775
4	3.5	0.839187	0.787737
5	4	0.843846	0.792111
6	4.5	0.843907	0.792168
7	5	0.415216	0.238727

Table 7

FIGURE CAPTIONS

Fig. 1. (a) Component diagram (Ejector Expansion Refrigeration System), (b) Ejector Expansion Refrigeration System p – h diagram.
Fig. 2. Ejector Geometry.
Fig. 3. Ejector Mesh View
Fig. 4. ER Vs PCA Plot
Fig. 5. ER Vs PDA Plot
Fig. 6. ER Vs SCA Plot
Fig.7. ER Vs PDA Plot

International Journal of Environmental Sciences
ISSN: 2229-7359
Vol. 11 No. 23s, 2025
https://www.theaspd.com/ijes.php

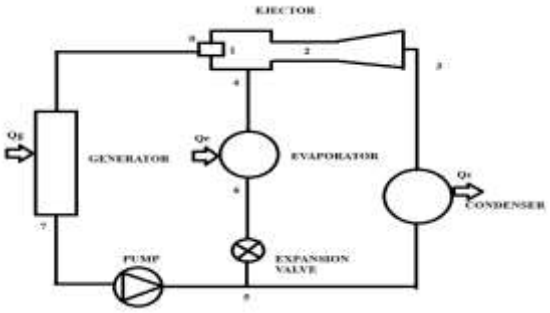

Fig. 1(a)

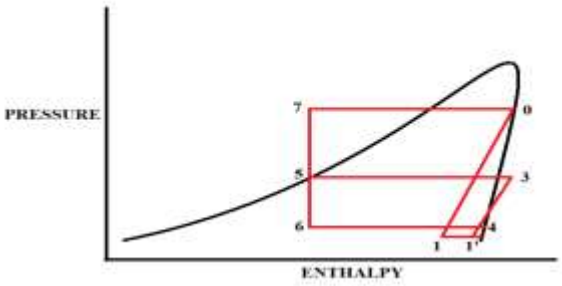

Fig. 1(b)

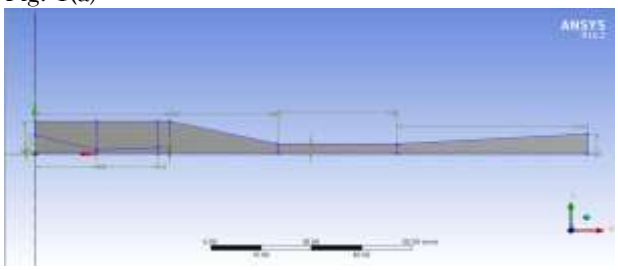

Fig. 2

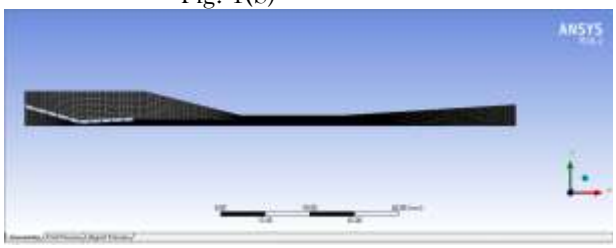

Fig. 3

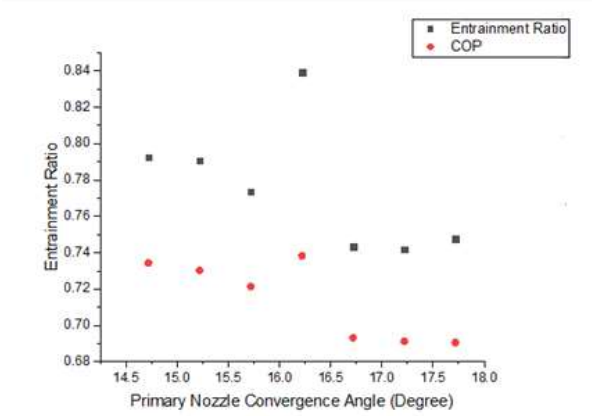

Fig. 4

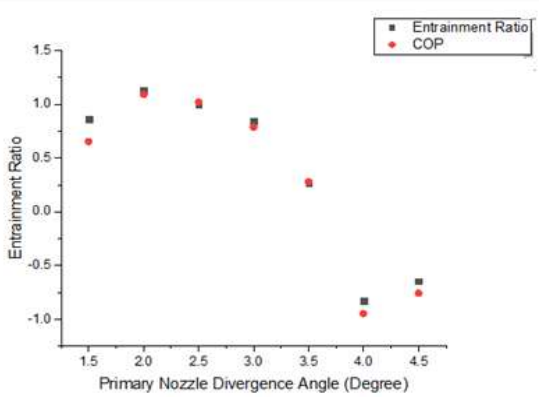

Fig. 5

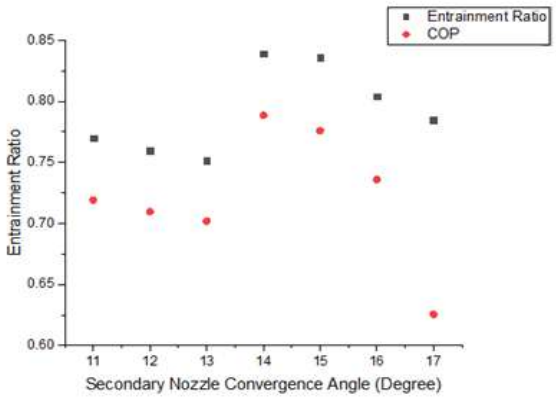

Fig. 6

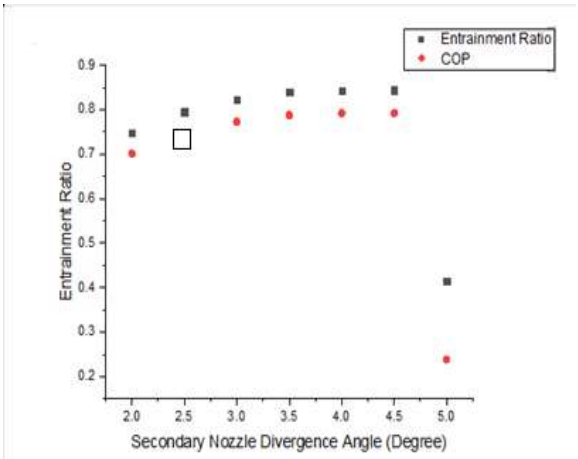

Fig. 7